Army Research Laboratory

A Novel Method for Generating Non-Stationary Gaussian Processes for Use in Digital Radar Simulators

by James A. Boehm and Patrick S. Debroux

ARL-TR-4051 March 2007

Army Research Laboratory

White Sands Missile Range, NM 88002-5513

ARL-TR-4051 **March 2007**

A Novel Method for Generating Non-Stationary Gaussian Processes for Use in Digital Radar Simulators

James A. Boehm and Patrick S. Debroux
Survivability/Lethality Analysis Directorate

REPORT DOCUMENTATION PAGE

Form Approved
OMB No. 0704-0188

1. REPORT DATE *(DD-MM-YYYY)*
March 2007

2. REPORT TYPE
Final

3. DATES COVERED (From - To)

4. TITLE AND SUBTITLE
A Novel Method for Generating Non-Stationary Gaussian Processes for Use in Digital Radar Simulators

5a. CONTRACT NUMBER

5b. GRANT NUMBER

5c. PROGRAM ELEMENT NUMBER

6. AUTHOR(S)
James A. Boehm and Patrick S. Debroux

5d. PROJECT NUMBER

5e. TASK NUMBER

5f. WORK UNIT NUMBER

7. PERFORMING ORGANIZATION NAME(S) AND ADDRESS(ES)
U.S. Army Research Laboratory
Information & Electronic Protection Division
Survivability/Lethality Analysis Directorate ATTN: AMSRD-ARL-SL-ES
White Sands Missile Range, NM 88002-5513

8. PERFORMING ORGANIZATION REPORT NUMBER
ARL-TR-4051

9. SPONSORING/MONITORING AGENCY NAME(S) AND ADDRESS(ES)
U.S. Army Research Laboratory
2800 Powder Mill Road
Adelphi, MD 20783-1197

10. SPONSOR/MONITOR'S ACRONYM(S)

11. SPONSOR/MONITOR'S REPORT NUMBER(S)
ARL-TR-4051

12. DISTRIBUTION/AVAILABILITY STATEMENT
Approved for public release; distribution is unlimited.

13. SUPPLEMENTARY NOTES

14. ABSTRACT
This report presents a novel and simple way to determine the transient response of the output of any linear system, described in the s-domain by an nth order polynomial, subjected to white Gaussian noise. The transient response of the output of the linear system is observed, in this report, in the variance of the output as a function of time. In addition, the mean and probability density function of the output are obtained. These results let simulation engineers create stable, unstable, and periodic stochastic processes for evaluation of communication and radar systems.

15. SUBJECT TERMS
Transient noise process, Fokker-Planck equation, Prediction

16. SECURITY CLASSIFICATION OF: a. REPORT	b. ABSTRACT	c. THIS PAGE	17. LIMITATION OF ABSTRACT	18. NUMBER OF PAGES	19a. NAME OF RESPONSIBLE PERSON
U	U	U	SAR	18	Patrick S. Debroux

19b. TELEPHONE NUMBER (*Include area code*)
505-678-5238

Standard Form 298 (Rev. 8/98)
Prescribed by ANSI Std. Z39.18

Contents

List of Figures

INTENTIONALLY LEFT BLANK.

1. Introduction

All filters in radar system simulations are normally assumed to be at steady state when subjected to deterministic and stochastic signals (the transient response has passed). The simulation usually uses some multiple of the step time-response constant to determine when the system enters steady state. This report shows a novel way to determine when steady state has been reached when subjected to stochastic signals. The steady state is defined as when the variance of the output has reached 95% of its steady state value.

The description of the transient response of a system subjected to noise is found in the solution for the probability density function of the process $V_{out}(t)$ described by the stochastic differential equation

$$\frac{d^n V_{out}}{dt^2} + a_{n-1}\frac{d^{n-1}V_{out}}{dt^{n-1}} + ... + a_0 V_{out} = V_{in}(t) \tag{1}$$

where the forcing function $V_{in}(t)$ is any stationary stochastic process.

The stochastic differential equation under this general forcing function does not have a closed-form solution. As in most cases, to make the solution tractable, we assume that the forcing function is a Gaussian distributed (stationary) stochastic process.

2. Theory

The transducer function $H(s)$ for an n^{th} order low pass filter in the s-domain (*1*) is

$$\frac{1}{2}\sqrt{\frac{R_2}{R_1}\frac{V_{in}(s)}{V_{out}(s)}} = s^n + a_{n-1}s^{n-1} + ... + a_0 \tag{2}$$

For ease of analysis we set the term $\frac{1}{2}\sqrt{\frac{R_2}{R_1}} = 1$. Under this assumption, equation 2 represents the left side of equation 1 in the s-domain.

Assuming $V_{in}(t)$ is a random voltage with a spectral density $W_0(f) = W_0$, then equation 1 becomes the general n^{th} order equation of the Langevin type. The solution for the probability density function for $V_{out}(t)$ using the Fokker-Planck equation found in Risken (*2*) is difficult. However, D'Azzo and Houpis (*3*) offer a closed-form solution to the problem if we convert equation 1 into an equivalent system of first-order differential equations.

In order to use the solution offered by D'Azzo and Houpis (*3*) (p.155), we transform equation 1 by first defining the operator $D^j = \frac{d^j}{dt^j}$, and then defining the phase variables in terms of this operator we obtain

$$x_1 = V_{out},\ x_2 = \dot{x_1} = DV_{out},\ ...,\ x_n = \dot{x}_{n-1} = D^{n-1}V_{out} \tag{3}$$

Using the phase variables, equation 1 can be written as a system of N first-order differential equations.

$$\dot{x} = \begin{bmatrix} 0 & 1 & & & & & \\ & 0 & 1 & & & 0 & \\ & & 0 & 1 & & & \\ & & & 0 & \ddots & & \\ & 0 & & & \ddots & & \\ & & & & & 0 & 1 \\ -a_0 & -a_1 & -a_2 & -a_3 & \cdots & a_{n-2} & a_{n-1} \end{bmatrix} x + \begin{bmatrix} 0 \\ 0 \\ 0 \\ 0 \\ 0 \\ 0 \\ 1 \end{bmatrix} V_{out} \tag{4}$$

From Risken (*2*) (section 3.2), equation 4 represents an Ornstein-Uhlenbeck process where the ξ variables have replaced the x variables and

$$\gamma = \begin{bmatrix} 0 & 1 & & & & & \\ & 0 & 1 & & & 0 & \\ & & 0 & 1 & & & \\ & & & 0 & \ddots & & \\ & 0 & & & \ddots & & \\ & & & & & 0 & 1 \\ -a_0 & -a_1 & -a_2 & -a_3 & \cdots & a_{n-2} & a_{n-1} \end{bmatrix} \tag{5}$$

Letting $V_{out}(t)$ have a zero-mean value, and since the noise is white, we have ${}_{out}(t)V_{out}(t')\rangle = D\delta(t-t')$ for the correlation function

$$q = \begin{bmatrix} 0 & & & & & \\ & 0 & & & 0 & \\ & & 0 & & & \\ & & & \ddots & & \\ & & & & 0 & \\ & 0 & & & 0 & \\ & & & & & D \end{bmatrix} \tag{6}$$

where D is the power spectral noise density of the white Gaussian process $V_{in}(t)$.

From Risken (*2*) (p.153) we learn that the drift coefficient is linear in the Ornstein-Uhlenbeck process. Note that Risken (*2*) uses the Einstein summation convention for the Latin indices but not for Greek indices. We will do the same.

$$D_i = -\gamma_{ij} x_j \tag{7}$$

The diffusion coefficient is a constant, that is

$$\gamma_{ij},\ D_{ij} = D_{ji} \qquad \text{(Constant matrix)} \tag{8}$$

Following Risken (*2*), for the derivation of the solution for the transition probability density, we determine the complete biorthogonal set for the γ matrix,

$$\gamma_{ij} u_j^{(\alpha)} = \lambda_a u_j^{(\alpha)};\quad \gamma_{ij} \nu_i^{(\alpha)} = \lambda_a \nu_j^{(\alpha)} \tag{9}$$

with the orthonormality and completeness relation

$$\sum_a \nu_i^{(\alpha)} u_j^{(\alpha)} = \delta_{ij};\quad u_i^{(\alpha)} \nu_i^{(\beta)} = \delta_{\alpha\beta} \tag{10}$$

Such a complete biorthogonal set exists if the N eigenvalues are all different.

The spectral decomposition of the matrix γ is

$$\gamma_{ij} = \sum_\alpha \lambda_\alpha u_i^{(\alpha)} \nu_j^{(\alpha)} \tag{11}$$

and we have

$$G_{ij}(t) = \left[e^{-\gamma t)}\right]_{ij} = \sum_\alpha e^{-\lambda_\alpha t} u_i^{(\alpha)} \nu_j^{(\alpha)} \tag{12}$$

Using Risken (*2*) (eq. 6.118) for the matrix σ

$$\sigma_{ij}(\tau) = 2D_{ks} \cdot \int_0^{\tau} G_{ik}(\tau')G_{js}(\tau')d\tau' \tag{13}$$

we obtain

$$\sigma_{ij}(t) = 2\sum_{\alpha,\beta} \frac{1 - e^{-(\lambda_\alpha+\lambda_\beta)t}}{\lambda_\alpha + \lambda_\beta} D^{(\alpha,\beta)} u_i^{(\alpha)} u_j^{(\beta)} \tag{14}$$

where

$$D^{(\alpha,\beta)} = \nu_k^{(\alpha)} D_{kl} \nu_l^{(\beta)} \tag{15}$$

By using equations 7-14 and performing the integration (explained in Risken (*2*), section 2.3.3), we arrive at the expression for the transition probability density function

$$\begin{aligned} P(\{x\}, t|\{x'\}, t') &= \left(\frac{2}{\pi}\right)^{-\frac{N}{2}} [Det\ \sigma(t-t')]^{-\frac{1}{2}} \\ &\cdot \ exp \begin{pmatrix} l - \frac{1}{2}[\sigma^{-1}(t-t')]_{ij}[x_i - G_{jk}(t-t')x_k'] \\ \cdot [x_j - G_{jl}(t-t')x_l'] \end{pmatrix} \end{aligned} \tag{16}$$

To solve equation 16 in closed-form will require closed-form solutions for the eigenvalues of γ and for the inverse of the σ matrix (*4*). Modern symbolic processors can accomplish this, but it will prove very difficult for a symbolic processor to integrate out the $(n-1)$ variables to obtain the probability density function for x. If this closed-form is obtained, an additional integration will be required to obtain the mean and variance of the variable x.

Since the joint probability density function is Gaussian, the mean, variance, and probability density function can be obtained from the characteristic function. Since the D matrix contains only one constant element, the expressions for the mean, variance, and probability density function of x can be simplified.

From Middleton (*5*) (section 7.3) we see that the mean and correlation matrices in terms of the variables in Risken (*2*) (eq 6.113) for the characteristic function (keeping with the Einstein summation convention) can be expressed as sums. This step is necessary so that symbolic and numerical calculations can be performed.

$$mean = M_i(t-t') = G_{ij}(t-t')x'_j = \sum_{\alpha} e^{-\lambda_\alpha t} u_i^{(\alpha)} \nu_j^{(\alpha)} x'_j \tag{17}$$

where the x'_j are the initial conditions for the random variable x_j(at $t = t'$) for the differential equation for the probability density function (Risken (*2*) (eqs. 16.108, 16.109).

$$K = \sigma_{ij} = 2\sum_{\alpha,\beta} \frac{1-e^{-(\lambda_\alpha+\lambda_\beta)t}}{\lambda_\alpha+\lambda_\beta} \left(\nu_k^{(\alpha)} D_{kl} u_j^{(\beta)}\right) u_i^{(\alpha)} \nu_j^{(\beta)} \tag{18}$$

Using equation 17 we obtain for the mean of the variable x_1

$$M_{x1} = \sum_{k=1}^{N} G_{1k} x_k = \sum_{k=1}^{N} \sum_{j=1}^{N} e^{-\lambda_j t} u_1^k \nu_j^k x_k \tag{19}$$

Using equation 18 we obtain for the variance of variable x_1

$$Var_1 = o_{11}(t) = 2\sum_{\alpha,\beta} \frac{1-e^{-(\lambda_\alpha+\lambda_\beta)t}}{\lambda_\alpha+\lambda_\beta} \left(\nu_N^{(\alpha)} D_{N,N} u_N^{(\beta)}\right) u_1^{(\alpha)} \nu_1^{(\beta)} \tag{20}$$

From Middleton (*5* p.16) we have the result that the marginal characteristic function corresponding the marginal probability density function for x_1 is just the joint characteristic function with all the k_s, except k_1 is set equal to zero. Thus the marginal characteristic function for x_1 is

$$mcf_{x1} = e^{-iM_{x1}k_1 + 0_{11}k_1^2} \tag{21}$$

Taking the inverse Fourier transform of equation 19 we obtain the marginal probability density function for the variable x_1. Using the fact that the joint probability density function is Gaussian and the properties of the joint characteristic function, we can obtain the mean and variance of the variable x_1 by simple summation, and the marginal probability density function by a single one-dimensional Fourier transform.

3. Comparison of Simulation and Theoretical Results

To compare simulation and theoretical results of the means, variances and marginal probability density function for the variable x_1, second-, third-, and fourth-order

Butterworth transfer function were used. The 3dB cutoff frequency in all three cases was $\omega = 1$. To obtain the simulation results, 4,000 representations of the non-stationary stochastic process x_1 were generated. The value of D used was 2.5 and the initial condition for x_1 was 2.

A relationship between the value of D used in the theoretical results and the variance of the Gaussian noise source used in the simulation has to be established. The D_{theo} used in the theoretical results is one half the noise density obtained by dividing the total power by the bandwidth. The noise density used in the simulation is the variance (total power) of the Gaussian noise generator divided by the simulation bandwidth. Thus, the simulation noise density is $(D_{sim} - \sigma_{sim})\delta t$, where the simulation sample time is δt. Since the two D's must be the same, we have

$$\sigma_{sim} = \frac{2D_{theo}}{\delta t} \tag{22}$$

Figures 1 and 2 show the analytical and simulated results for the mean as a function of time.

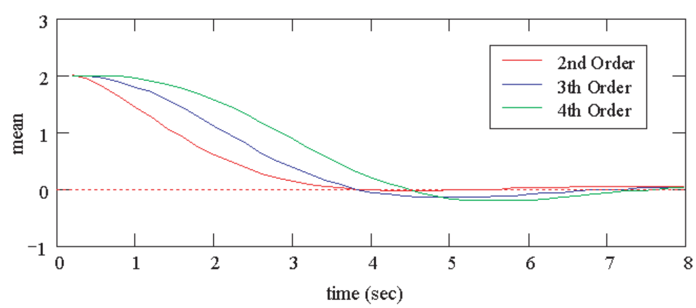

Figure 1. Analytical results for the means.

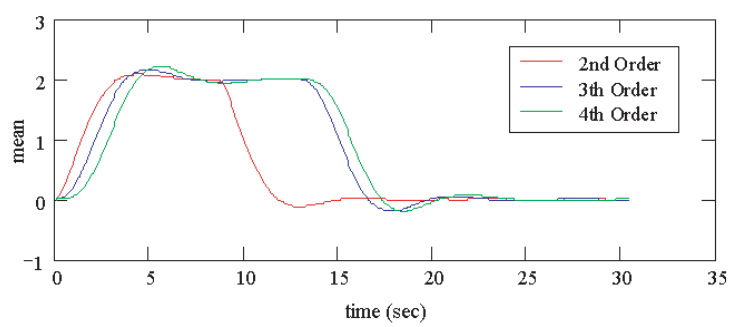

Figure 2. Simulation results for the means.

Figure 1 shows the expected result that the transient response of the filter increases as the order of the filter is increased.

The simulation results agree with the theoretical results. Note that the higher the order of the filter, the longer it takes to reach steady state. In order to simulate the initial condition for the stochastic variable x_1, it was necessary to drive the filter with a direct current (DC) voltage equal to the initial condition x_1' and then let the output of the filter reach the steady state value x_1'. When steady state was reached, the stationary Gaussian process (D = 2.5) was applied to the input of the filter.

To show just how close the simulation was to theoretical values, the simulation results are overlaid the theoretical for the third order filter in figure 3. The simulation results are shifted in time to match the theoretical.

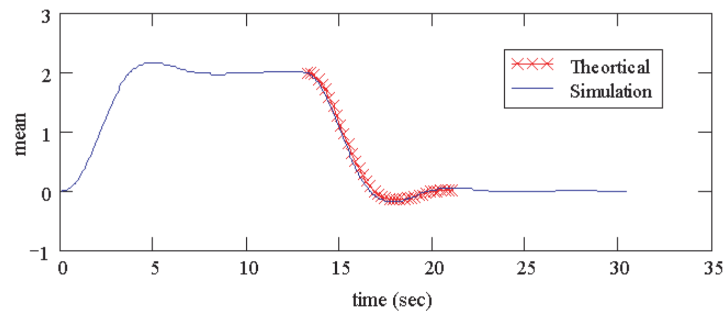

Figure 3. Comparisons of results for the mean for the third-order Butterworth filter response.

Figures 4 and 5 show the analytical and simulation results for the variance as a function of time.

Both figures 4 and 5 show that as the order of the filter is increased, the time for the variance of the output to reach steady state increases.

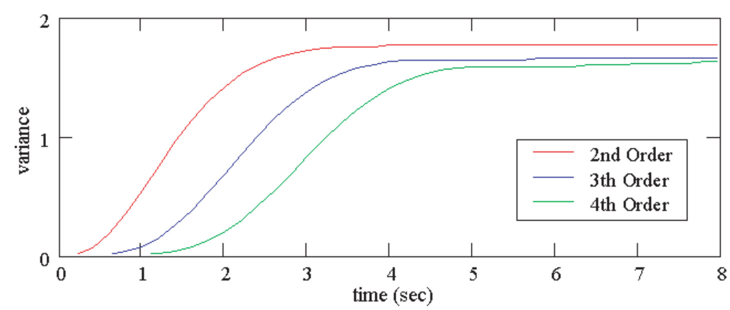

Figure 4. Analytical results for the variances.

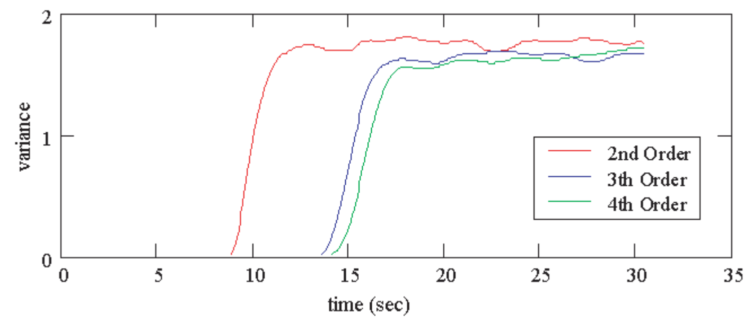

Figure 5. Simulation results for the variances.

As in the mean calculations, in order to simulate the initial condition for the variable x_1, the output of the filter, it was necessary to drive the filter with the initial condition voltage and let it stabilize to the initial condition. Again, at the stabilization time the stationary Gaussian process (D = 2.5) was applied.

To show just how close the simulation is to theoretical values of settling time of the variance, the simulation results for the third-order filter are superimposed on the analytical in figure 6. Again, the results were shifted in time to compare the simulation against the analytical results.

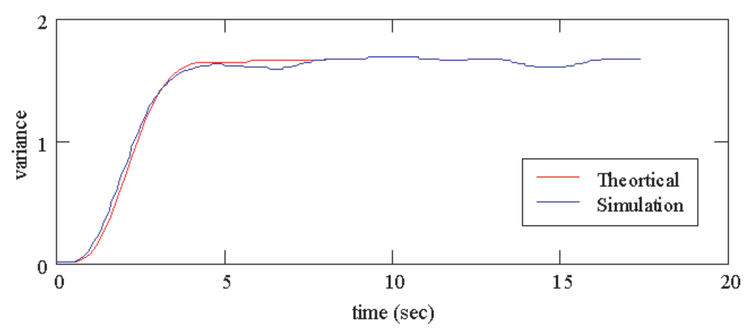

Figure 6. Comparison of results for the variances for the third-order Butterworth filter response.

Figure 6 shows that we have a very close match between simulates and analytical in the transient response of the variance.

Figure 7 shows the theoretical probability density function for as a function of four time values.

Figure 8 shows simulation and theoretical results for the probability density function of x_1 for two values of time.

Figure 8 shows that the theoretical and simulation histograms are in good agreement.

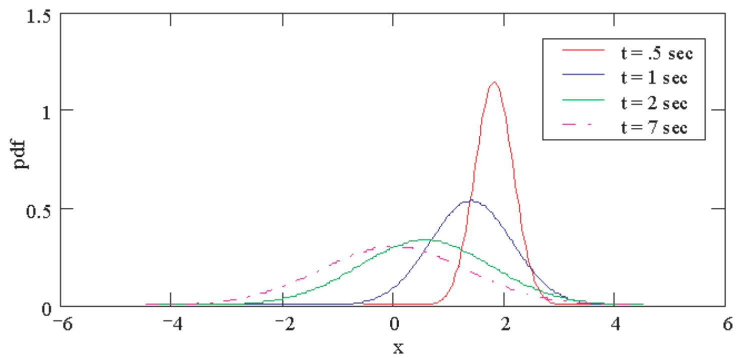

Figure 7. Theoretical probability density for the third-order Butterworth filter response.

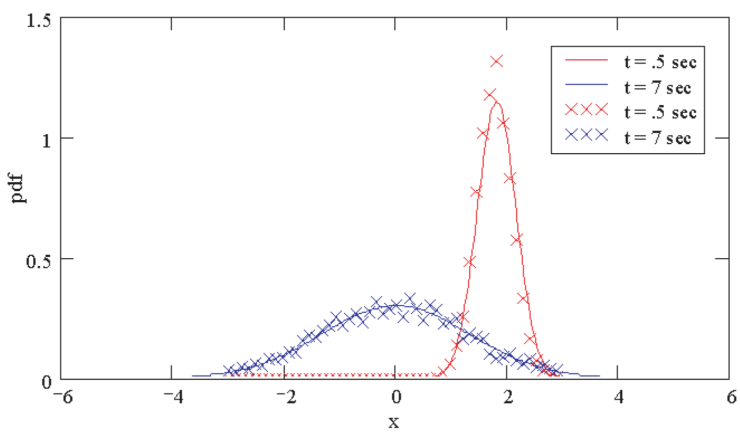

Figure 8. Theoretical probability density and simulation for the third-order Butterworth filter response.

Figure 9 shows the theoretical step response and variance as a function of time for a third-order Butterworth filter. The step response is amplitude scaled so that both plots approach the same steady state value.

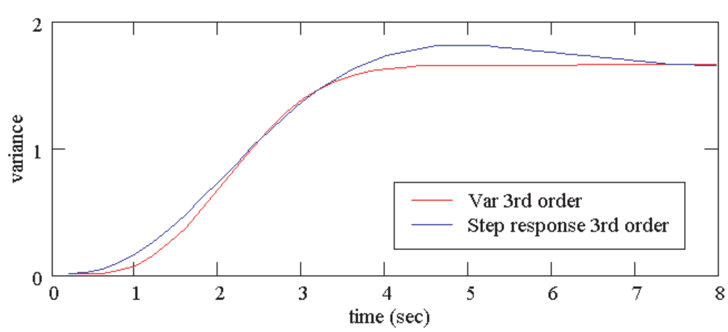

Figure 9. Variance of the step function input response of a third-order Butterworth filter.

Figure 9 shows that for the third-order system that the time for both the variance and step response to approach steady state are of the same order. This is important because we see that steady state, as measured by the variances, is reached before the classic definition of steady state for a deterministic input. This allows the step response for complex systems to be used as a measure of the transient response of the complex system to stochastic processes.

Does this hold in general? Since both responses are control by the eigenvalues, a heuristic argument indicates it does. A mathematical argument will have to wait for a later report.

4. Conclusions

We have shown that the simulation and predicted results are in very close agreement with each other when calculating the transient response of a stable low pass filter output. The theory shows that we are not limited to this case only. We can easily create unstable Gaussian processes. By varying the initial conditions in a periodic manner we can create stable and unstable periodic Gaussian processes for use in evaluating communication and radar simulations.

Soong (*6*) shows how to extend the results of this report to the case where the processes are not white noise defined by Soong (*6*), equation 7.199.

$$dY(t) = g(Y(t), t)dt + dB(t) \tag{23}$$

The limitation of this analysis is in not showing the exact relationship between the step response to filters described by equation 2 and the transient response of the variance of the output for this class of filters. This is needed to use the easily obtained step response as an upper bound for the transient of the variance of the output of the filter.

References

[1] Temens, Gabor C; Mitars, Sanjit K. Eds. *Modern Filter Theory and Design*, John Wiley & Sons: New York, 1973; ISBN 0-471-85130-2.

[2] Risken, H. *The Fokker-Planck Equation Methods of Solution and Applications*, Second Edition, Springer-Verlag: Berlin, 1989; ISBN 0-387-50498-2.

[3] D'Azzo, John J. Constantine H. Houpis, *Linear Control System Analysis and Design Conventional and Modern*, McGraw-Hill: New York, 1988; ISBN 0-07-016186-0.

[4] Zverev, Anotol I. *Handbook of Filter Synthesis*, John Wiley & Sons: New York, 1967; ISBN 0-471-98680-1.

[5] Middleton, David *Introduction to Statistical Communication Theory*, Peninsula Publishing: Los Altos, CA., 1987; ISBN 0-932146-5.

[6] Soong, T. T. *Random Differential Equations in Science and Engineering*, Academic Press: New York, 1973; ISBN 72-84372.

Distribution List

US ARMY RESEARCH LAB 1
ATTN IMNE ALC IMS A SMITH
MAIL & RECORDS MGMT
ADELPHI MD 20783-1197

ADMNSTR 1 electronic
DEFNS TECHL INFO CTR
ATTN DTIC OCP ELECT CPY V MADDOX
8725 JOHN J KINGMAN RD STE 0944
FT BELVOIR VA 22060-6218

US ARMY RESEARCH LAB 2
AMSRD ARL CI OK TL TECHL LIB
ATTN K RAPKA
2800 POWDER MILL ROAD
ADELPHI MD 20783-1197

US ARMY RESEARCH LAB 2
AMSRD CI OK TP TECHL LIB
ATTN T LANDFRIED
APG MD 21005

US ARMY RESEARCH LAB 1
ATTN AMSRD MAILROOM VAULT R REYNA
BLDG 1624
WSMR NM 88002-5513

US ARMY RESEARCH LAB 1
AMSRD ARL SL
ATTN P TANENBAUM
APG MD 21005

US ARMY RESEARCH LAB 1
AMSRD ARL SL E
ATTN R FLORES
BLDG 1624
WSMR NM 88002-5513

US ARMY RESEARCH LAB 10
ATTN AMSRD ARL SL ES
J GONZALEZ
E JACKSON
G VILLALVA
R VEGA
J BOEHM (3)
P DEBROUX (3)
BLDG 1624
WSMR NM 88002-5513

US ARMY RESEARCH LAB 1
AMSRD ARL SL EE
ATTN E REDE
BLDG 1624
WSMR NM 88002-5513

TOTAL 20